Hindawi Publishing Corporation
Journal of Nanomaterials
Volume 2016, Article ID 5646175, 7 pages
http://dx.doi.org/10.1155/2016/5646175

Research Article

Photocatalytic Reduction Activity of {001} TiO_2 Codoped with F and Fe under Visible Light for Bromate Removal

Yan Zhang,[1] Lingdan Li,[1] and Hongyuan Liu[2]

[1]*Department of Civil Engineering, Zhejiang University, 866 Yuhangtang Road, Hangzhou 310058, China*
[2]*College of Civil Engineering and Architecture, Zhejiang University of Technology, 18 Chaowang Road, Hangzhou 310014, China*

Correspondence should be addressed to Hongyuan Liu; lhyzyy@zjut.edu.cn

Received 19 August 2016; Revised 25 October 2016; Accepted 1 November 2016

Academic Editor: Ramasamy Karvembu

The presence of bromate in water is a well-known problem because of its toxic effects on human health, particularly its carcinogenic potential. Photocatalytic reduction is an attractive process for bromate removal. F- and Fe-codoped TiO_2 (F-Fe-TiO_2) with a {001} facet was successfully prepared, and its bromate-removal activity under visible light was examined. The microstructure, morphology, and chemical state of the doping elements and the optical property of the photocatalysts were examined using transmission electron microscopy (TEM), X-ray photoelectron spectroscopy (XPS), electron paramagnetic resonance (EPR), photoluminescence spectroscopy (PLS), and UV-Vis diffuse reflectance spectra (DRS). The results indicate that the optical properties of F-Fe-TiO_2 with the {001} facet and cuboid morphology were obviously improved and its photocatalytic activity was significantly enhanced. The bromate solution of 100 μg/L was thoroughly removed with 0.5 g/L dosage of 1.0% F- and 0.08% Fe-codoped TiO_2 composite within 1 hour under visible light.

1. Introduction

As a disinfection byproduct, bromate generally originates from bromide-containing water during the ozonation or chlorination process [1, 2]. As an International Agency for Research on Cancer (IARC) classified group B-2 substance [3], bromate is limited to the maximum contaminant level (MCL) of 10 μg/L by the World Health Organization (WHO) and United States Environmental Protection Agency (USEPA) [2]. Appropriate technologies are imminently required for bromate removal to ensure the safety of water. The current alternatives to remove bromate are physical adsorption methods [4], biological treatment [5], catalytic reduction [6–9], electrochemical reduction [10], and photocatalysis [11, 12].

Compared to other methods, photocatalysis has advantages in terms of high efficiency and stability without secondary pollution [13]. Because of its photochemical stability, nontoxicity, and low cost, titanium dioxide has been widely investigated in water treatment and air pollution control as a photocatalyst [14]. However, the unfavourable photocatalytic efficiency and limitation of visible-light usage hinder the practical application of titanium dioxide. The key to overcoming these limitations is to improve the band gap, which is responsible for the optical response and separation of photogenerated electrons and holes [15]. Several methods are available for enhancing the photocatalytic efficiency of TiO_2, such as surface sensitization [16], noble-metal deposition [17], composite semiconduction [18], and metal or non-metal element doping [19].

Codoped TiO_2 has been demonstrated as an outstanding method to satisfy practical requirements because of its synergistic effects. Similar to the photocatalyst codoped with metallic and nonmetallic elements, the optical properties are significantly improved because of the respective contributions and collaborative strengthening from the two types of elements. Therefore, the key is to find suitable metallic and nonmetallic elements. Xin et al. [20] prepared Fe^{3+}-doped TiO_2, which performed much better than Degussa P25. Fe^{3+} can capture the photoinduced electrons, inhibit the recombination of photoinduced electron-hole pairs, and narrow the band gap. Yang and coworkers [21] prepared TiO_2 with a high percentage of the {001} crystal phase using HF as the crystal control agent. The surface free energy of the {001}

crystal phase is relatively high in anatase TiO_2. Higher surface free energy of the crystal surface corresponds to higher photocatalytic activity, improving the optical performance of the photocatalyst. Considering the improved light response range and inhibition of electron-hole pair recombination as a result of Fe doping and the enhanced photocatalytic activity as a result of F doping, F- and Fe-codoped TiO_2 may be a promising material for bromate removal.

A series of F- and Fe-codoped TiO_2 samples were prepared and characterized in this study. The photocatalytic reduction activities of the samples for bromate removal were examined. The mechanism of the photocatalytic reaction is also discussed.

2. Experimental Section

2.1. Materials. Chemically pure tetrabutyl titanate (TBT) and analytical grade iron(III) nitrate nonahydrate ($Fe(NO_3)_3 \cdot 9H_2O$), ethyl alcohol (C_2H_5OH), and hydroflu-oric (HF) acid were used to synthesize F- and Fe-codoped TiO_2 nanoparticles. Sodium bromate (>99.7%) was used to prepare the bromate solution. All chemicals were purchased from the Sinopharm Chemical Reagent (Shanghai, China).

2.2. Synthesis of F-Fe-TiO_2. The codoped F-Fe-TiO_2 particles were prepared using a one-step hydrothermal reaction with TBT as the titanium source and hydrofluoric (HF) acid as the crystal control agent. First, 15 mL of TBT was added to the Polytetrafluoroethylene (PTFE) linings of a stainless-steel reaction vessel. Then, appropriate amounts of HF and $Fe(NO_3)_3 \cdot 9H_2O$ were added. The mixtures were maintained for 24 h at 180°C, and the hydrothermal reaction occurred. After cooling to room temperature, the precursors were washed several times with distilled water and an ethanol solution. The white precipitates were completely dried at 60°C and ground into powders for future use. The final powders were expressed as xF-yFe-TiO_2, where x and y are the molar ratios of $F : TiO_2$ (%) and $Fe : TiO_2$ (%), respectively. Different molar ratios of x (0.5–2.0%) and y (0.03–0.2%) were prepared for the experiments in this work.

2.3. Characterization of Samples. The surface microstructure and morphology of the F-Fe-TiO_2 samples were characterized using an H-9500 transmission electron microscope (TEM, Hitachi, Japan). The surface compositions and binding energies of the samples were determined using an Escalab X-ray photoelectron spectroscope (XPS, VG, UK) and a Bruker A300 electron paramagnetic resonance spectrometer (EPR, Bruker, Germany). The combination of the photoinduced electrons and holes was observed in the photoluminescence spectra (PLS) using an FLS920 fluorescence spectrophotometer (FLS, Edinburgh Instruments, UK) at room temperature and an excitation wavelength λ_{ex} of 260 nm. The light response capability of the photocatalysts was obtained from the TU1901 UV-Vis diffuse reflectance spectra (DRS, Beijing Purkinje, China).

Table 1: Analytical conditions for ion chromatograph to determine anions.

Instrument	Dionex-2000
Analytical column	Dionex IonPac AS19 (4 × 250 mm)
Guard column	Dionex IonPac AG19 (4 × 250 mm)
Detection	Suppressed conductivity
Suppressor	Dionex Anion Self-Regenerating Suppressor (Dionex ASRS 300 4 mm), AutoSuppression Recycle Mode
Eluent solution	20 mM KOH
Carrier gas	1.0 mL/min N_2

2.4. Batch Experiments. Unless specifically mentioned, 0.5 g/L F-Fe-TiO_2 samples were added to a double-glazing reactor, which was filled with 400 mL of 100 μg/L bromate solution. Before the photocatalytic reaction, the reactor was stirred using a magnetic stirrer in the dark for 0.5 h to reach adsorption equilibrium. The photoreaction of bromate was performed under a 50 W high-pressure mercury lamp for 1 h with a UV cut-off filter (through $\lambda > 420$ nm) to ensure the irradiation of visible light. At predetermined time intervals, the samples were collected to determine the concentrations of bromate and bromide with a Dionex ICS2000 ion chromatograph, and the analytical conditions for ion chromatograph can be seen in Table 1. Unless otherwise specified, the experiments were conducted with 1.0F-0.08Fe-TiO_2, pH, temperature, and initial bromate concentration of 0.5 g/L, 4.3, 298 K, and 100 μg/L, respectively. All experiments were performed in triplicate.

3. Results and Discussion

3.1. Morphology Characterization. Figure 1 shows the TEM images of doped TiO_2. In addition to circular particles, cubic 1.0F-0.08Fe-TiO_2 with edges and corners were observed. The cubic morphology originates from the F doping [21] because 1.0F-TiO_2 also has a cube structure, whereas 0.08Fe-TiO_2 is only spherical. Because F was added in trace amount, the morphology control of the photocatalyst was not complete. The size of cubic 1.0F-0.08Fe-TiO_2 was 10–30 nm along the diagonal of the cubes, which is smaller than that of the other two samples. Moreover, lattice spacing of 0.235 nm was revealed from the high-resolution transmission electron microscopy (HRTEM) image in Figure 1(b). This result indicates the existence of {001} crystal [22] and further confirms the successful control of the crystal surface.

3.2. Existing Forms of F and Fe. The XPS result (Figure 2) shows the elemental composition of F-Fe-TiO_2. The major peaks are F1s, O1s, Ti2s, Ti2p, and Ti3p. The C1s peak may be derived from the hydrothermal products of the TBT structure [23]. Meanwhile, a clear peak at approximately 685 eV suggests the presence of F, which corresponds to the peak of the Ti-F bond that formed on the surface. Hence, F was successfully doped onto the TiO_2 particle, which is consistent with the TEM results in Figure 1. No Fe peak was found possibly because of the low Fe amount.

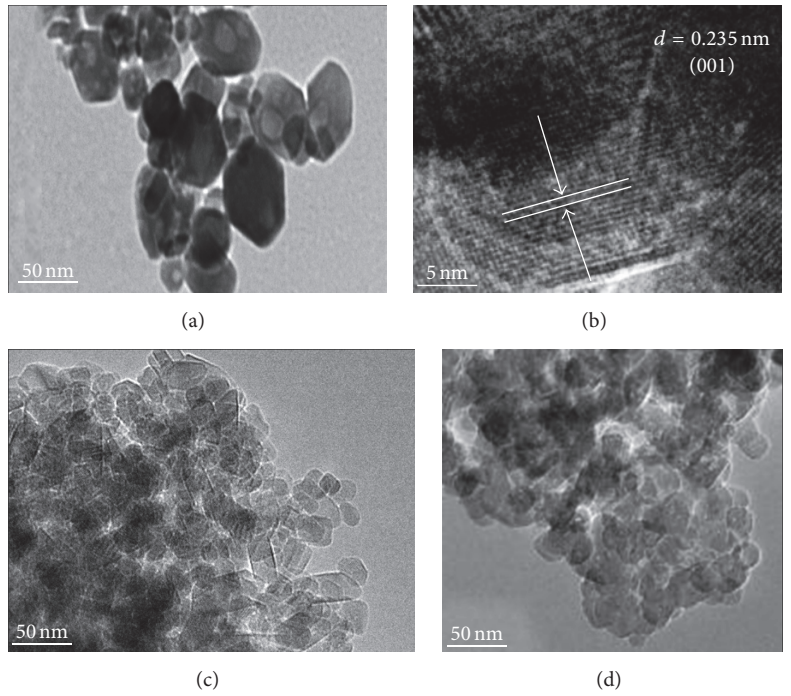

Figure 1: TEM images of (a) 1.0F-0.08Fe-TiO_2, (c) 1.0F-TiO_2, and (d) 0.08Fe-TiO_2; (b) HRTEM image of 1.0F-0.08Fe-TiO_2.

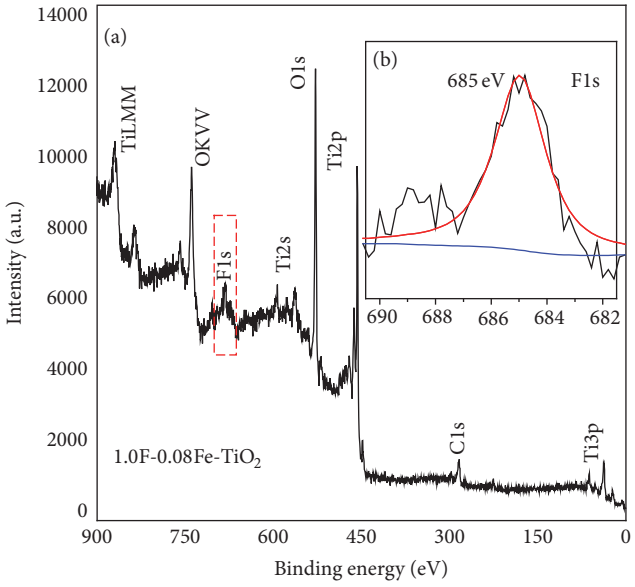

Figure 2: XPS of F-Fe-TiO_2.

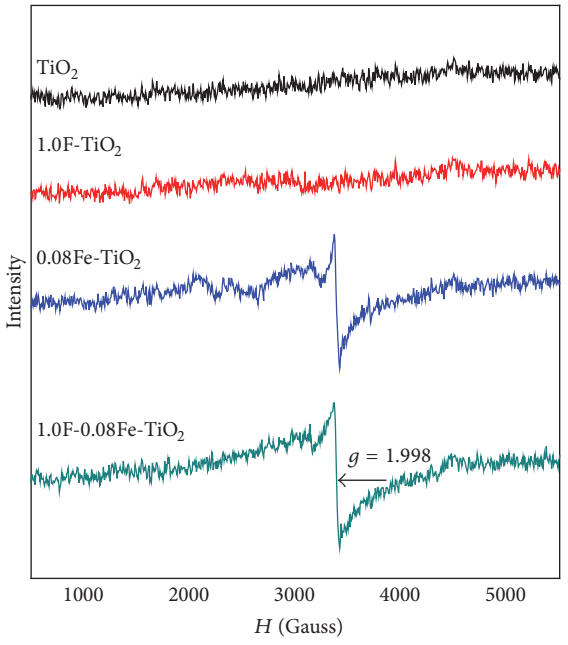

Figure 3: EPR spectra of TiO_2 and doped TiO_2 at room temperature.

EPR spectroscopy was used to study the existing forms of Fe. EPR is a highly sensitive technique to examine paramagnetic species, even when the Fe levels are less than 0.01%. Compared to TiO_2 and 1.0F-TiO_2 (Figure 3), there is an obvious signal of paramagnetic species at $g = 1.998$ in the Fe-TiO_2 and F-Fe-TiO_2 samples, which can be ascribed to Fe^{3+}-substituted Ti^{4+} in the TiO_2 lattice [24, 25]. Moreover, the Fe peak in F-Fe-TiO_2 is broadened and has a higher intensity than Fe-TiO_2. The reason for this occurrence may be the increase in relative intensity of the EPR signal with the decrease in sample size, which is consistent with the results that some smaller particles are found in the TEM characterization of F-Fe-TiO_2.

3.3. Characterization of Optical Properties. The effect of F and Fe codoping on the recombination of photogenerated

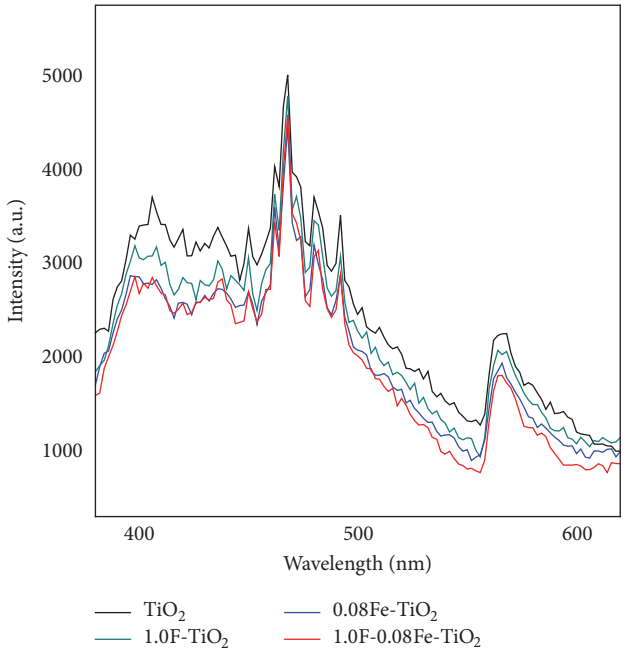

Figure 4: PLS of TiO_2 and doped TiO_2 excited by monochromatic light (260 nm) at room temperature.

electron-hole pairs of TiO_2 was measured based on the PLS. As shown in Figure 4, the PL intensities of Fe-TiO_2 and F-Fe-TiO_2 are lower than that of TiO_2, particularly F-Fe-doped TiO_2. Thus, the recombination of the electron-hole pairs is effectively restrained because of the synergistic effects of F and Fe.

To identify the light absorption of the composites, UV-Vis diffuse reflectance spectra, as shown in Figure 5, were analysed. With the doping of F or Fe, the absorption values increase at wavelengths longer than 400 nm. As estimated in Figure 5(b), the band gap energy of Fe-TiO_2 and F-Fe-TiO_2 is approximately 2.55 eV, which is much narrower than that of F-TiO_2 and TiO_2 (2.92 eV). Hence, the visible-light photoresponse was enhanced and the band gap energy was narrowed as a result of Fe doping; F-Fe-TiO_2 can work in the visible range [26].

As previously mentioned, the results indicate that the optical properties of F-Fe-TiO_2 are significantly enhanced and may be favourable for the improvement of its photocatalytic activity, which is subsequently discussed.

4. Photocatalytic Properties

Figure 6(a) shows the results of bromate reduction by codoped TiO_2 with various molar ratios of F : TiO_2 and Fe : TiO_2 under visible light. The ordinate represents the bromate-removal ratio. The bromate-removal ratio is obviously related to the molar ratios of F : TiO_2 and Fe : TiO_2. The molar ratio of Fe : TiO_2 has a stronger effect on the bromate-removal ratio than that of F : TiO_2. A possible reason for this occurrence is that the doped Fe in TiO_2 can effectively capture the photoinduced electrons and narrow the band gap to expand the range of light response. However, the introduction of F can control the generation of the {001} facet, impel electrons to migrate to the {101} facet with lower energy to join the bromate reduction, and cause the holes to assemble on the {001} facet [22]. Therefore, codoped F and Fe can inhibit recombination of the photoelectron-hole pairs and induce more photogenerated electrons and holes to participate in the photocatalytic reactions. Moreover, nearly 100% bromate removal in 1 h was observed for the 1.0F-0.08Fe-TiO_2 photocatalysis.

Table 2: Bromine species during bromate reduction by F-Fe-TiO_2.

Item	C_0	$C_{0.5\,h}$	$C_{1\,h}$	$C_{1.5\,h}$	$C_{2\,h}$	$C_{2.5\,h}$
BrO_3^- (μmol/L)	0.78	0.21	0	0	0	0
Br^- (μmol/L)	0	0.32	0.57	0.68	0.71	0.71
Total (μmol/L)	0.78	0.53	0.57	0.68	0.71	0.71

Figure 6(b) shows the photocatalytic bromate reduction by TiO_2 and doped TiO_2, where C_0 is the initial bromate concentration (μg/L) and C is the concentration at time t (μg/L). This figure shows that nearly 100% of the bromate (from an initial concentration of 0.78 μmol/L) was removed by F-Fe TiO_2 in 1 h, whereas only 56% and 27% removal ratios were obtained for F-TiO_2 and Fe-TiO_2, respectively. This result further verifies the synergy of F and Fe on bromate reduction, which is consistent with the optical-property characterization results.

Photocatalyst dosage plays an important role in the absorption of light and bromate; thus, experiments on photocatalytic bromate reduction at different F-Fe-TiO_2 doses were performed; the results are shown in Figure 7. The optimal removal efficiency was obtained with a dosage of 0.5 g/L, likely because the light irradiation was hindered by the excessive catalyst, which remained suspended in the solution and affected the reaction.

To further explore the transformation process of bromate removal, a bromine balance test was performed. The bromate and bromide concentrations and the total bromine mass are shown in Table 2. During the photocatalysis process, the bromide (Br^-) concentration increased when BrO_3^- was reduced. The bromate removal by F-Fe-TiO_2 possibly occurs by a two-step mechanism. First, bromate in the solution adsorbs onto the photocatalyst surface. Then, bromate is reduced by the electron from F-Fe-TiO_2 to bromide. Because the adsorption of bromine is approximately ten percent of the ratio on the catalyst, bromide is the only reduced product after 2 h of photocatalytic reaction.

5. Conclusions

F- and Fe-codoped TiO_2 particles were successfully prepared using a one-step hydrothermal method. The batch experimental studies suggest that an initial bromate concentration of 100 μg/L can be completely removed by 0.5 g/L 1.0F-0.08Fe-TiO_2 nanoparticles under visible light in 1 h. Codoping of F and Fe can significantly improve the catalytic properties of TiO_2 because of the contributions of each element

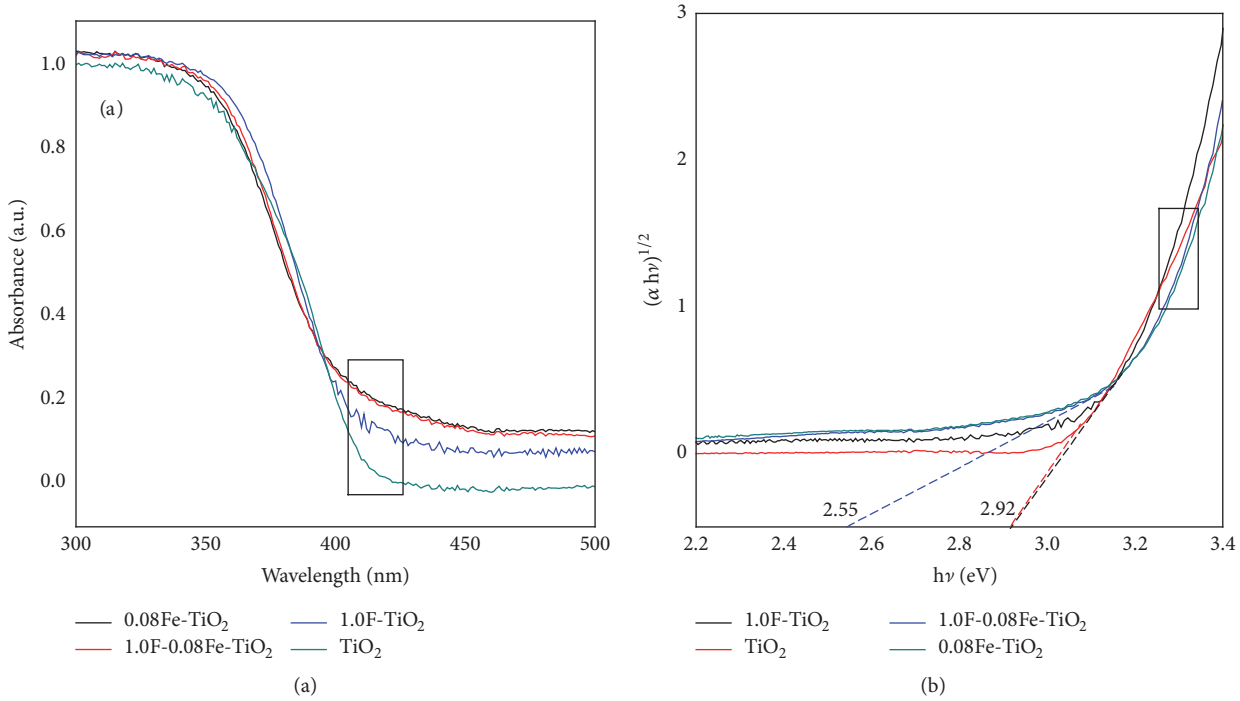

Figure 5: (a) UV-Vis DR spectra of TiO_2 and doped TiO_2 particles; (b) plot of the transformed Kubelka-Munk function versus light energy.

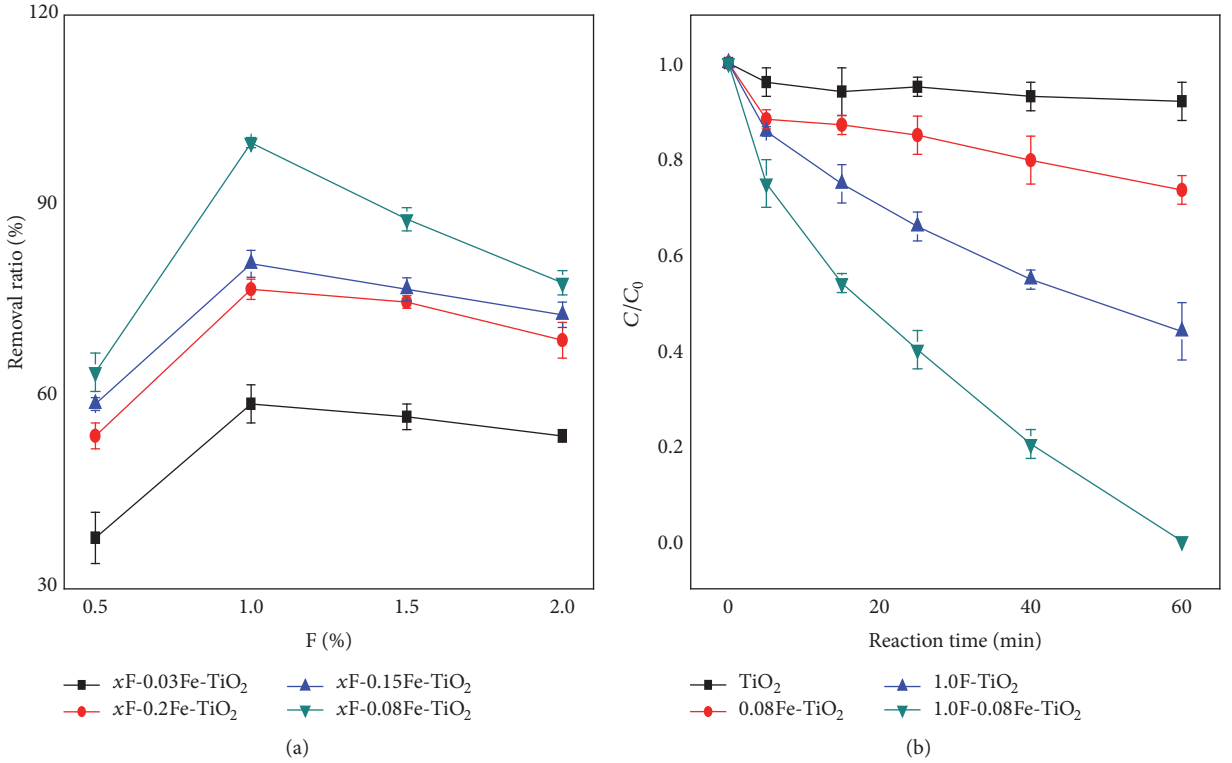

Figure 6: (a) Effect of molar ratios of F : TiO_2 and Fe : TiO_2 on photocatalytic bromate reduction; (b) typical curves of bromate removal by TiO_2 and doped TiO_2.

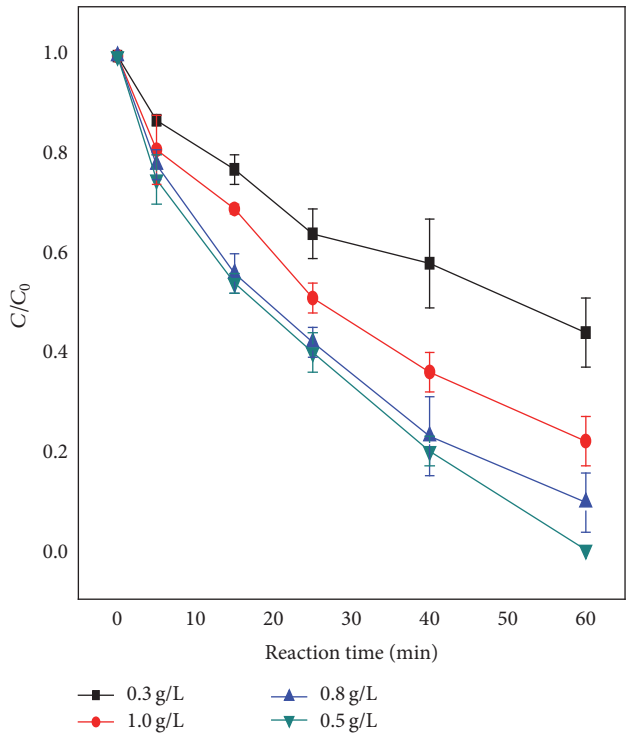

FIGURE 7: Effect of F-Fe-TiO_2 dosage on bromate reduction.

and their synergism. The recombination of photoelectron-hole pairs is remarkably inhibited by the generation of the {001} facet as a result of the F doping and electron transfer function of Fe. The band gap of 1.0F-0.08Fe-TiO_2 is narrowed from 2.92 to 2.55, which expands the range of light response. Because of this notable performance enhancement, F-Fe-TiO_2 is a potential material for the removal of bromate from water.

Competing Interests

The authors declare that they have no competing interests.

Acknowledgments

This research was supported by the National Science and Technology Major Project of China: Water Pollution Control and Treatment (2012ZX07403-003).

References

[1] U. Von Gunten, "Ozonation of drinking water: part I. Oxidation kinetics and product formation," *Water Research*, vol. 37, no. 7, pp. 1443–1467, 2003.

[2] H. S. Weinberg, C. A. Delcomyn, and V. Unnam, "Bromate in chlorinated drinking waters: occurrence and implications for future regulation," *Environmental Science and Technology*, vol. 37, no. 14, pp. 3104–3110, 2003.

[3] M. M. Moore and T. Chen, "Mutagenicity of bromate: implications for cancer risk assessment," *Toxicology*, vol. 221, no. 2-3, pp. 190–196, 2006.

[4] M. J. Kirisits, V. L. Snoeyink, and J. C. Kruithof, "The reduction of bromate by granular activated carbon," *Water Research*, vol. 34, no. 17, pp. 4250–4260, 2000.

[5] R. Butler, A. Godley, L. Lytton, and E. Cartmell, "Bromate environmental contamination: review of impact and possible treatment," *Critical Reviews in Environmental Science and Technology*, vol. 35, no. 3, pp. 193–217, 2005.

[6] D. B. Thakur, R. M. Tiggelaar, Y. Weber, J. G. E. Gardeniers, L. Lefferts, and K. Seshan, "Ruthenium catalyst on carbon nanofiber support layers for use in silicon-based structured microreactors. Part II: catalytic reduction of bromate contaminants in aqueous phase," *Applied Catalysis B: Environmental*, vol. 102, no. 1-2, pp. 243–250, 2011.

[7] J. Restivo, O. S. G. P. Soares, J. J. M. Órfão, and M. F. R. Pereira, "Metal assessment for the catalytic reduction of bromate in water under hydrogen," *Chemical Engineering Journal*, vol. 263, pp. 119–126, 2015.

[8] J. Restivo, O. S. G. P. Soares, J. J. M. Órfão, and M. F. R. Pereira, "Bimetallic activated carbon supported catalysts for the hydrogen reduction of bromate in water," *Catalysis Today*, vol. 249, pp. 213–219, 2015.

[9] H. Zhang, R. Deng, H. Wang et al., "Reduction of bromate from water by zero-valent iron immobilized on functional polypropylene fiber," *Chemical Engineering Journal*, vol. 292, pp. 190–198, 2016.

[10] N. Kishimoto and N. Matsuda, "Bromate ion removal by electrochemical reduction using an activated carbon felt electrode," *Environmental Science and Technology*, vol. 43, no. 6, pp. 2054–2059, 2009.

[11] X. Huang, L. Wang, J. Zhou, and N. Gao, "Photocatalytic decomposition of bromate ion by the UV/P25-Graphene processes," *Water Research*, vol. 57, pp. 1–7, 2014.

[12] X. Zhao, H. Liu, Y. Shen, and J. Qu, "Photocatalytic reduction of bromate at C_{60} modified Bi_2MoO_6 under visible light irradiation," *Applied Catalysis B: Environmental*, vol. 106, no. 1-2, pp. 63–68, 2011.

[13] X. Zhang, T. Zhang, J. Ng, J. H. Pan, and D. D. Sun, "Transformation of bromine species in TiO_2 photocatalytic system," *Environmental Science and Technology*, vol. 44, no. 1, pp. 439–444, 2010.

[14] K. Nagaveni, G. Sivalingam, M. S. Hegde, and G. Madras, "Photocatalytic degradation of organic compounds over combustion-synthesized nano-TiO_2," *Environmental Science and Technology*, vol. 38, no. 5, pp. 1600–1604, 2004.

[15] L. Cui, Y. Wang, M. Niu, G. Chen, and Y. Cheng, "Synthesis and visible light photocatalysis of Fe-doped TiO_2 mesoporous layers deposited on hollow glass microbeads," *Journal of Solid State Chemistry*, vol. 182, no. 10, pp. 2785–2790, 2009.

[16] X. Luo, C. Zha, and B. Luther-Davies, "Photosensitivity of titania-doped hybrid polymer prepared by an anhydrous sol-gel process," *Optical Materials*, vol. 27, no. 8, pp. 1461–1466, 2005.

[17] H. Einaga, T. Ibusuki, and S. Futamura, "Improvement of catalyst durability by deposition of Rh on TiO_2 in photooxidation of aromatic compounds," *Environmental Science and Technology*, vol. 38, no. 1, pp. 285–289, 2004.

[18] J. D. Bryan, S. M. Heald, S. A. Chambers, and D. R. Gamelin, "Strong room-temperature ferromagnetism in Co^{2+}-doped TiO_2 made from colloidal nanocrystals," *Journal of the American Chemical Society*, vol. 126, no. 37, pp. 11640–11647, 2004.

[19] E. A. Reyes-Garcia, Y. Sun, K. Reyes-Gil, and D. Raftery, " ^{15}N solid state NMR and EPR characterization of N-doped TiO_2

photocatalysts," *Journal of Physical Chemistry C*, vol. 111, no. 6, pp. 2738–2748, 2007.

[20] B. Xin, Z. Ren, P. Wang, J. Liu, L. Jing, and H. Fu, "Study on the mechanisms of photoinduced carriers separation and recombination for Fe^{3+}-TiO_2 photocatalysts," *Applied Surface Science*, vol. 253, no. 9, pp. 4390–4395, 2007.

[21] H. G. Yang, C. H. Sun, S. Z. Qiao et al., "Anatase TiO_2 single crystals with a large percentage of reactive facets," *Nature*, vol. 453, no. 7195, pp. 638–641, 2008.

[22] N. Roy, Y. Sohn, and D. Pradhan, "Synergy of low-energy {101} and high-energy {001} TiO_2 crystal facets for enhanced photocatalysis," *ACS Nano*, vol. 7, no. 3, pp. 2532–2540, 2013.

[23] B. Erdem, R. A. Hunsicker, G. W. Simmons, E. D. Sudol, V. L. Dimonie, and M. S. El-Aasser, "XPS and FTIR surface characterization of TiO_2 particles used in polymer encapsulation," *Langmuir*, vol. 17, no. 9, pp. 2664–2669, 2001.

[24] Y. Cong, J. Zhang, F. Chen, M. Anpo, and D. He, "Preparation, photocatalytic activity, and mechanism of nano-TiO_2 Co-doped with nitrogen and iron (III)," *The Journal of Physical Chemistry C*, vol. 111, no. 28, pp. 10618–10623, 2007.

[25] K. Nagaveni, M. S. Hegde, and G. Madras, "Structure and photocatalytic activity of $Ti_{1-x}M_xO_{2\pm\delta}$(M = W, V, Ce, Zr, Fe, and Cu) synthesized by solution combustion method," *Journal of Physical Chemistry B*, vol. 108, no. 52, pp. 20204–20212, 2020.

[26] D.-G. Huang, S.-J. Liao, J.-M. Liu, Z. Dang, and L. Petrik, "Preparation of visible-light responsive N–F-codoped TiO_2 photocatalyst by a sol–gel-solvothermal method," *Journal of Photochemistry and Photobiology A: Chemistry*, vol. 184, no. 3, pp. 282–288, 2006.